Transactions on Modelling and Simulation vol 22, © 1999 WIT Press, www.witpress.com, ISSN 1743-355X

Radial basis functions with compactly support and multizone decomposition: applications to environmental modelling

S. M. Wong[1,2], Y. C. Hon[1], and T. S. Li[2]
[1]*Department of Mathematics, City University of Hong Kong*
E-mail: maychon@cityu.edu.hk
[2]*School of Science and Technology, Open University of Hong Kong*
E-mail: anwong@ouhk.edu.hk, tsli@ouhk.edu.hk

Abstract
This paper presents the application of the radial basis functions (RBF) for solving a set of non-linear hydrodynamics model for marine environments. Two different techniques, namely compact support and multizone decomposition, are used to improve the conditioning of the resultant coefficient matrix which is a full matrix due to the use of the global radial basis functions. The idea of the compactly supported radial basis function (CSRBF) is to reduce the full matrix to a banded sparse matrix. The multizone approach is similar to the commonly used domain decomposition. The resulting sparse or smaller matrix has shown to improve in both stability and computational efficiency. Both techniques are verified by comparing with the global multiquadric radial basis function applied to a linear and a real non-linear two-dimensional hydrodynamic model in simulating the tidal current and water flow circulation patterns.

1 Introduction

The present study aims to simulate the spatial and temporal variation of tidal currents and water velocities in marine environments. Water quality monitoring programs are often limited in their extend of coverage both spatially and temporally. In light of the complicated interaction between the hydrological and physical processes, mathematical modellings which are commonly used to cope with complicated systems are considered to be practically valid for the prediction of future events. The application of Multiquadric(MQ) scheme for simulating water pollutants was found to be better in terms of numerical accuracy and rate of convergence than that of the fi-

Transactions on Modelling and Simulation vol 22, © 1999 WIT Press, www.witpress.com, ISSN 1743-355X

nite element scheme [1]. However MQ is a globally supported function and will generate a system of equations with a full coefficient matrix. Solving problems with full coefficient matrix is extremely expensive when the number of interpolation points reaches several hundreds. It will also result in instability and ill-conditioning.

To improve the forementioned problems, we propose to use compact support and multizone decomposition to work together with RBFs. The multizone approach is similar to domain decomposition which subdivide the whole domain into a number of non-overlapping finite zones. The resulting matrix for the computation of each local zone contains a much smaller number of data points. The compact support approach enables the RBFs scheme to generate banded sparse matrices.

Section 2 gives the description of the hydrodynamic equations. Section 3 introduces the application of RBFs with compact support and multizone decomposition. Numerical and computational results are presented in Section 4. The paper concludes with a discussion in Section 5.

2 Hydrodynamics Model for Fluid Velocities

The governing equations are the 2-dimensional depth-integrated version of three differential equations, namely the continuity equation and the momentum conservation equations in the x and y directions respectively in a region Ω. These equations are expressed in vector notation as:

$$\frac{\partial \boldsymbol{\Phi}}{\partial t} + \frac{\partial \boldsymbol{G}}{\partial x} + \frac{\partial \boldsymbol{F}}{\partial y} + \boldsymbol{E} = 0, \quad \text{in } \Omega \subset \boldsymbol{R}^2 \tag{2.1}$$

where $\boldsymbol{\Phi}$, $\boldsymbol{G}$, $\boldsymbol{F}$, $\boldsymbol{E}$ are column vectors given as below

$$\boldsymbol{\Phi} = \begin{bmatrix} \zeta \\ u \\ v \end{bmatrix} \quad \boldsymbol{G} = \begin{bmatrix} uH \\ u^2 \\ uv \end{bmatrix} \quad \boldsymbol{F} = \begin{bmatrix} vH \\ uv \\ v^2 \end{bmatrix}$$

$$\boldsymbol{E} = \begin{bmatrix} 0 \\ g(\frac{\partial \zeta}{\partial x} + \frac{u\sqrt{u^2+v^2}}{HC_b^2}) - fv - \frac{\rho_a}{H\rho_w} C_s W_x W_s \\ g(\frac{\partial \zeta}{\partial y} + \frac{v\sqrt{u^2+v^2}}{HC_b^2}) + fu - \frac{\rho_a}{H\rho_w} C_s W_y W_s \end{bmatrix}$$

where u, v are the depth-averaged advective velocities in x, y directions respectively; ζ is the sea water surface elevation; h is the mean depth of sea level; H is the total depth of sea level, such that $H = h + \zeta$; W_x, W_y are the wind velocity components in x, y directions respectively, and W_s is the wind speed given as $W_s = \sqrt{W_x^2 + W_y^2}$. C_b is the Chezy bed roughness coefficient; f is the coriolis force parameter; g is the gravitational acceleration; ρ_a is the density of air; ρ_w is the density of water and C_s is the surface friction coefficient.

The water boundary condition is defined as $\zeta(x, y, t) = \zeta^*(x, y, t)$, where $\zeta^*(x, y, t)$ is the specific sea surface elevation level on the water boundary.

The land boundary condition is defined as $\vec{Q} \cdot \vec{n} = 0$, where $\vec{Q}$ represents the velocity vector (u, v), $\vec{n}$ is the direction of the outward normal vector on the land boundary. At the n^{th} time step, the current velocities (u^n, v^n) on the land boundary are derived from this condition as

$$u^n(x_i, y_i) = \tilde{u}^n(x_i, y_i)\sin^2(\theta_i) - \tilde{v}^n(x_i, y_i)\sin(\theta_i)\cos(\theta_i)$$
$$v^n(x_i, y_i) = \tilde{v}^n(x_i, y_i)\cos^2(\theta_i) - \tilde{u}^n(x_i, y_i)\sin(\theta_i)\cos(\theta_i) \quad (2.2)$$

where $\tilde{u}^n(x_i, y_i)$ and $\tilde{v}^n(x_i, y_i)$ are the n time step values computed at data point (x_i, y_i) on the land boundary from the given interpolant, θ_i is the outward normal angles at the land boundary points which are computed by taking the average of the vectors joining the neighbouring points.

The initial conditions are $\vec{Q}(x_i, y_i, 0) = \vec{0}$, $\zeta(x_i, y_i, 0) = 0$, for all $(x_i,\ y_i)$ $\in \Omega$.

3 Radial Basis Functions

The theory of the RBF approximation have been discussed comprehensively in [3]. The principle idea of the radial basis interpolation is to interpolate a finite series of an unknown function $f(\boldsymbol{X})$ at N distinct points $\boldsymbol{X}_j$ on Ω by the following expansion

$$f(\boldsymbol{X}) \simeq \sum_{j=1}^{N} \alpha_j \phi(\|\ \boldsymbol{X} - \boldsymbol{X}_j\ \|), \quad (3.3)$$

where $\phi(\|\ \boldsymbol{X} - \boldsymbol{X}_j\ \|)$ is a radial basis function, $\boldsymbol{X}_j \in \boldsymbol{R}^n$, $j = 1, 2, \ldots, N$, $\|\ \boldsymbol{X} - \boldsymbol{X}_j\ \| = \boldsymbol{r}_j$ is the Euclidean distance, and α_j's are the unknown coefficients to be calculated. The most popular RBFs are Multiquadric $(\boldsymbol{r}_j^2 + c^2)^{1/2}$, thin plate spline $\boldsymbol{r}_j^c \log \boldsymbol{r}_j$, and Gaussian $e^{-c\boldsymbol{r}_j^2}$ where $c \neq 0$. These functions are globally supported.

To solve the two-dimensional time-dependent differential equations given in equations (2.1), it is integrated in time using explicit forward difference scheme given as

$$\boldsymbol{\Phi}_i^{n+1} = \boldsymbol{\Phi}_i^n - \Delta t\left(\frac{\partial \boldsymbol{G}_i^n}{\partial x} + \frac{\partial \boldsymbol{F}_i^n}{\partial y} + \boldsymbol{E}_i^n\right), \quad (3.4)$$

where Δt is the time step, $\boldsymbol{\Phi}_i^{n+1}$ is the solution vector at the points (x_i, y_i) in time $n\Delta t$. The values of the interpolant $\boldsymbol{\Phi}^n$ are given by the following radial basis function

$$\boldsymbol{\Phi}^n(x_i, y_i) = \sum_{j=1}^{N} \boldsymbol{\alpha}_j^n \phi(\sqrt{(x_i - x_j)^2 + (y_i - y_j)^2}), \quad (3.5)$$

which are collocating with a set of data points $(x_i, y_i)_{i=1}^N$ over the domain $\Omega \subset \boldsymbol{R}^2$. This equation forms a system of N linear equations in N unknowns which can be expressed in matrix form

$$A\vec{\boldsymbol{\alpha}} = \vec{\boldsymbol{\Phi}}, \quad (3.6)$$

where $A = [\phi_j(x_i, y_i)]$ is a $N \times N$ coefficient matrix; $\vec{\boldsymbol{\alpha}} = [\boldsymbol{\alpha}_j^n]$ and $\vec{\boldsymbol{\Phi}} = [\boldsymbol{\Phi}_j^n]$ are $N \times 1$ matrices. The unknown coefficients vector $[\boldsymbol{\alpha}_j^n]$ can be determined using Gaussian elimination.

Transactions on Modelling and Simulation vol 22, © 1999 WIT Press, www.witpress.com, ISSN 1743-355X

It follows that the numerical values for the corresponding spatial derivatives $\frac{\partial \Phi^n(x_i,y_i)}{\partial x}$ and $\frac{\partial \Phi^n(x_i,y_i)}{\partial y}$ can be calculated using equation (3.5). The solution of the variables (ζ, u, v) is solved by substituting the partial derivatives into the equation (3.4) with the given boundary conditions.

Compact support and multizone decomposition techniques are introduced here to make the RBF approximation more feasible for the solving large scale problems. The algorithm of these two schemes gives a chance to reduce the computational time and improve the stability of the computation by the reduction of the size of the coefficient matrix to be solved.

3.1 Compactly Supported Radial Basis Functions

Compactly supported radial basis functions (CSRBF) was firstly introduced by Wu [5] and later expanded by Wendland [4] in the mid 1990s. Floater and Iske [6] first adopted the CSRBFs for multi-step scattered data interpolation. Fasshauer [7, 8] then introduced a multilevel approximation scheme incorporated with CSRBF for the solution of boundary value problems and linear partial differential equations.

The principle idea of CSRBFs is to use a polynomial as a function of Euclidean distance r with support on [0, 1]. CSRBFs must be strictly positive definite in R^d for all d less than or equal to some fixed value d_0. The basic definition of the CSRBF $\phi_{l,k}(r)$ have the form

$$\phi_{l,k}(r) = (1-r)_+^n \, p(r), \quad \text{for } k \geq 1, \tag{3.7}$$

with the following conditions

$$(1-r)_+^n = \begin{cases} (1-r)^n & \text{if } 0 \leq r < 1; \\ 0 & \text{if } r \geq 1 \,, \end{cases}$$

where l is the dimension number, $2k$ is the smoothness of the function, $r = \| \boldsymbol{X} - \boldsymbol{X}_j \|$ is the Euclidean distance, $\boldsymbol{X}_j \in R^d$, $j = 1, 2, \ldots, N$, $p(r)$ is the prescribed polynomial.

Wendland's CSRBFs is adopted to replace the global basis function. For small number of $k = 0, 1, 2, 3$, Wendland's CSRBFs can be formulated explicitly in the form

$$\phi_{l,0}(r) \doteq (1-r)_+^l, \tag{3.8}$$

$$\phi_{l,1}(r) \doteq (1-r)_+^{l+1} \left[(l+1)r + 1\right], \tag{3.9}$$

$$\phi_{l,2}(r) \doteq (1-r)_+^{l+2} \left[(l^2+4l+3)r^2 + (3l+6)r + 3\right], \tag{3.10}$$

$$\begin{aligned}\phi_{l,3}(r) \doteq\; & (1-r)_+^{l+3} \left[(l^3+9l^2+23l+15)r^3\right. \\ & \left. + (6l^2+36l+45)r^2 + (15l+45)r + 15\right].\end{aligned} \tag{3.11}$$

For any given dimension d, the value l can be determined by $\lfloor \frac{d}{2} \rfloor + k + 1$. For instant, when $d = 3$, the Wendland's function in C^0, C^2, C^4 and C^6 can be expressed respectively in the following polynomials form

$$\phi_{2,0}(r) \doteq (1-r)_+^2, \tag{3.12}$$

$$\phi_{3,1}(r) \doteq (1-r)_+^4\,(4r+1), \tag{3.13}$$
$$\phi_{4,2}(r) \doteq (1-r)_+^6\,(35r^2+18r+3), \tag{3.14}$$
$$\phi_{5,3}(r) \doteq (1-r)_+^8\,(32r^3+25r^2+8r+1), \tag{3.15}$$

These functions have compact support on $[0,\ 1]$ and vanish on $[1,\ \infty]$. We can scale a basis function with compact support on $[0,\ \delta]$ by replacing r with $\frac{r}{\delta}$ where $\delta > 0$. With a scaling factor δ the interpolation function $\mathbf{\Phi}^n$ in the equation (3.5) is written as

$$\mathbf{\Phi}^n(x_i, y_i) = \sum_{j=1}^{N} \alpha_j^n \phi_{l,k}^{\delta}\left(\frac{r}{\delta_j}\right), \tag{3.16}$$

where $r = [(x_i - x_j)^2 + (y_i - y_j)^2]^{1/2}$, δ_j can be variable or constant for different node points depends on the nature of the problem. An important unsolved problem is to find a method to determine the optimal size of δ. In general, the smaller the value of δ, the higher percentage of zero entries. However, this would also be resulted in lower accuracy.

3.2 RBFs with Multizone Decomposition

Under the multi-zone decomposition scheme described in [2], the domain Ω is divided into K zones Ω^j, $j = 1, 2, \ldots, K$, hence the global set of interpolation points W is also divided into K subsets of data points W^j, $j = 1, \ldots, K$ such that $W^i \cap W^j = \emptyset$, for $i \neq j$ and $\bigcup_{i=1}^{K} W^i = W$.

For the zone Ω^k we denote the set of data points in it by $W^k = \{P_j^k \mid j = 1, 2, \ldots, L_k\}$ where L_k is the number of data point in subset W^k. Each subset W^k is assigned with approximately the same number of data points for an efficient load balancing computation.

In order to enhance the accuracy of computation of each zone and to maintain continuity of the interpolation function across the zones' boundaries, two more sets of extra data points will be put together with the data points in W^k. The first set includes all the points which are in other zones and adjacent to the boundary of Ω^k and is denoted as $B^k = \{P_j^k \in W^l \mid l \neq k \text{ and } j = L_k+1, L_k+2, \ldots, L_k+M_k,\}$, where M_k is the total number of data points considered to be close to the boundary of Ω^k and is relatively smaller than L_k. The second set of data points which are chosen at random such that they are sparsely and evenly distributed over the other zones in Ω. We denote this set of extra data points as $S^k = \{P_j^k \in W^l \mid l \neq k \text{ and } j = L_k+M_k+1, L_k+M_k+2, \ldots, L_k+M_k+N_k,\}$, where N_k is also a number relatively smaller than L_k.

To calculate the solution in each zone Ω_k, the calculation of the unknown coefficients α_i is applied to the data points in $W^k \cup B^k \cup S^k$ in a similar manner as global simulation. The basis interpolating function for zone K is given as

$$\mathbf{\Phi}_k{}^n(x_j, y_j) = \sum_{i=1}^{L_k+M_k+N_k} \alpha_i^n \phi([(x_j - x_i)^2 + (y_j - y_i)^2]^{1/2}), \tag{3.17}$$

where n denotes the n^{th} time step and $(x_j, y_j) \in (W^k \cup B^k \cup S^k)$. Having calculated the set of unknown coefficients $\boldsymbol{\alpha}_i$, for $i = 1, 2, \ldots, L_k + M_k + N_k$, the corresponding partial derivatives for the collocation points in subset W^k are calculated but not those in B^k and S^k. This is because the extra data points in B^k and S^k are from other zones, their partial derivative would be computed when the zone they belonged are to be considered.

When the numerical values $\boldsymbol{\Phi}(x_i, y_i)$ of the next time step $n+1$ are calculated using Equation (3.4), only local information of the points in W^k is required which have all been found in previous time steps.

4 Numerical Verifications and Results

To compare the efficiency and applicability of the methods, we apply the proposed schemes to solve a linear and a non-linear hydrodynamics models separately.

Case 1- Linear water flow equation

This linear shallow water equation is converted by neglecting the wind stress, bottom friction and the coriolis force terms from equations (2.1). This simple model allows a comparison of the computed results with the analytical solution. For the time integration scheme, we adopt the Euler method of second order which yields

$$\zeta^{n+1} = \zeta^n - \Delta t H \{\nabla \cdot \mathbf{V}\}^n + \frac{(\Delta t)^2}{2} Hg \left\{\nabla^2 \zeta\right\}^n, \tag{4.18}$$

$$\mathbf{V}^{n+1} = \mathbf{V}^n - \Delta t g \{\nabla \zeta\}^n + \frac{(\Delta t)^2}{2} Hg \left\{\nabla^2 \cdot \mathbf{V}\right\}^n. \tag{4.19}$$

where $\mathbf{V}$ is a vector of the depth-averaged advective velocities in x, y directions respectively. As shown in *Figure 1*, we generate 205 collocation points in a rectangular channel with length $L = 872km$, width $W = 50km$ and depth $H = 20m$, in which 117 collocation points are in the interior, 5 are on the water boundary and 83 are on the land boundary. The boundary conditions are:

$$\zeta(t) = \zeta_0 \cos \omega t, \text{ at } x = 0, \quad 0 \le y \le W, \tag{4.20}$$

$$u(t) = 0, \text{ at } x = L, \quad 0 \le y \le W, \tag{4.21}$$

$$v(t) = 0, \text{ at } y = 0, \text{ and } y = W, \quad 0 \le x \le W, \tag{4.22}$$

and the initial conditions are $\vec{Q}(x, y, 0) = \mathbf{0}$ and $\zeta(x, y, 0) = 0$, where $\zeta_0 = 1\,m$ and $\omega = 1.45444 \times 10^{-4}/s$. The analytical solution to this boundary-value problem is known and is given by

$$\zeta(x, y, t) = \zeta_0 \cos\left(\frac{\omega}{\sqrt{gH}}(L - x)\right) \frac{\cos \omega t}{\cos\left(\frac{\omega}{\sqrt{gH}} L\right)}; \tag{4.23}$$

$$u(x, y, t) = -\zeta_0 \sqrt{\frac{g}{H}} \sin\left(\frac{\omega}{\sqrt{gH}}(L - x)\right) \frac{\sin \omega t}{\cos\left(\frac{\omega}{\sqrt{gH}} L\right)}; \tag{4.24}$$

$$v(x, y, t) = 0. \tag{4.25}$$

Transactions on Modelling and Simulation vol 22, © 1999 WIT Press, www.witpress.com, ISSN 1743-355X

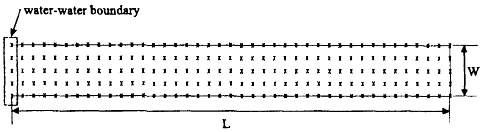

Figure 1: *A rectangular channel with 205 collocation points.*

The solution corresponds only to the interaction between the incident wave and the reflected wave from the wall at $x = L$. The results of Wendland's CSRBF $\phi^{\delta}_{4,2}(r)$ and 4-zones model are presented in *Table 1* for comparison. For example, CSRBF $\phi^{\delta}_{4,2}(r)$ for the interpolation of ζ can be written as

$$\zeta^n(x_i, y_i) = \sum_{j=1}^{N} \beta_j^n [(1 - \frac{r}{\delta_j})_+^6 (35(\frac{r}{\delta_j})^2 + 18\frac{r}{\delta_j} + 3)]. \tag{4.26}$$

Table 1 shows the root-mean-square (RMS) error of the tidal level (ζ) and water velocity (u) calculated by the proposed models in comparison with the analytical solution. All results are generated with time step $\Delta t = 30$ seconds.

We can see from the table that the level of accuracy of the CSRBFs decreased tremendously with decrease in scaling factor from 1.0×10^7 to 2.0×10^7. The results show that the computation of CSRBF is quite accurate even for a very sparse matrix due to the simplicity of the model.

Regarding computational efficiency, Multi-zone MQ performed more efficiently with a saving of 61% in CPU time comparing the same order of accuracy with the global MQ scheme, while CSRBF at $\delta = 2.0 \times 10^7$ saves only 43%.

Table 1. Results of Water velocity(u) and current(ζ)

	tidal level(ζ)			velocity(u)			CPU time
N	92	102	112	92	102	112	ratio (%)
$\phi^{\delta}_{4,2}(\frac{r}{\delta})$, $\delta = 2.0 \times 10^7$							57%
RMS error(cm)	0.70	0.32	0.35	0.46	0.38	0.49	(41% nonzeros
abs_max error(cm)	1.48	1.18	0.67	0.81	0.92	0.91	entry)
$\phi^{\delta}_{4,2}(\frac{r}{\delta})$, $\delta = 1.0 \times 10^7$							33%
RMS error(cm)	4.78	2.58	4.33	2.51	1.48	2.09	(20% nonzeros
abs_max error(cm)	8.49	5.95	4.73	4.42	4.04	4.57	entry)
Global MQ with $r = 0.815d_{min}$							
RMS error(cm)	0.49	0.71	1.01	0.63	1.0	1.48	100%
abs_max error(cm)	1.19	1.51	1.76	1.06	2.33	2.74	
4-zones MQ with $r = 0.815d_{min}$							
RMS error(cm)	0.67	0.74	1.45	0.54	1.14	1.32	39%
abs_max error(cm)	1.50	1.44	1.58	0.86	2.21	2.45	

Case 2 - Non-linear water flow equations

In this case, the application of the schemes is applied to a real-life model. We use Tolo Harbour of Hong Kong as a reference test case for the model described in Section (2). The embayment of Tolo Harbour occupies an area of $50\,km^2$ and is $16\,km$ long. The width of the embayment varies from $5\,km$ in the inner basin to just over $1\,km$ at the mouth of the channel

Harbour. The geographical conditions of the harbour are outlined in [1]. The construction of the RBFs schemes is based on the set of 260 data points as indicated in *Figure 2*.

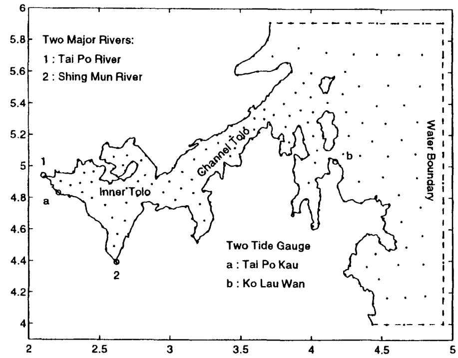

Figure 2: *The dots (•) distributed on the map represents the interpolation points.*

To satisfy the water boundary condition, the input surface elevation ζ^n on water-water boundary is estimated using the equation suggested by the Observatory of Hong Kong given as $\zeta^n(x_i, y_i, t) = \zeta^*(t + T_{COR_i}) + H_{COR_i}$ for $i = 1, 2, \cdots, 23$, where $\zeta^*(t)$ is the actual tide data measured at a tide gauge, T_{COR_i} is the time correction parameter, H_{COR_i} is the tide level correction parameter.

The multizone model is verified with 5-zones and 7-zones and compared to Wendland CSRBF $\phi^{\delta}_{3,1}$. The numerical experiments have shown that the degree of numerical accuracy of CSRBF has improved when a relatively larger value of scaling factor δ for the water boundary points is used compared to interior points. In fact, δ for these points were set large enough to cover the whole region in order to propagate the updated information in each time step. In this way, all the entries in the columns of the coefficient matrix corresponding to those water boundary points are non-zero. The remaining part of the matrix would still be banded.

The simulation is carried out for a total number of 1100 hours with time step size of 30 seconds. The numerical results are compared with the observed data collected at tide gauges of the harbour.

Table 2. The tidal level for the interpolation point at a tide gauge

	RMS error (m)	absolute Max. error (m)	CPU time ratio (%)
global MQ	7.41×10^{-2}	2.76×10^{-1}	100%
5 zones MQ	8.08×10^{-2}	2.22×10^{-1}	58%
7 zones MQ	7.31×10^{-2}	2.46×10^{-1}	48%
CSRBF, $\delta = 1.5 \times 10^6$	7.52×10^{-2}	2.74×10^{-1}	88% (78% nonzeros entry)
CSRBF, $\delta = 1.3 \times 10^6$	8.35×10^{-2}	2.55×10^{-1}	79% (69% nonzeros entry)
CSRBF, $\delta = 1.2 \times 10^6$	8.42×10^{-2}	2.74×10^{-1}	74% (64% non-zeros entry)

By comparing the root-mean-square errors, although the level of accuracy of the CSRBF model at $\delta = 1.5 \times 10^6$ is close to global MQ model, it only saves 12% of CPU times, while multizone model reduces a significant amount of computational times by 42% when compare with the global MQ results. The performance of multi-zone decomposition models exhibits reasonable stability and accuracy. The flooding velocities showed in *Figure 4* has indicated that the accuracy and smoothness in distribution of velocities can not be maintained as good as Multizone models. *Figure 3* shows the comparison of the computed tidal level for the period between 23 February 1991 and 27 February 1991 for the nodal point at Ko Lau Wan Tide Gauge.

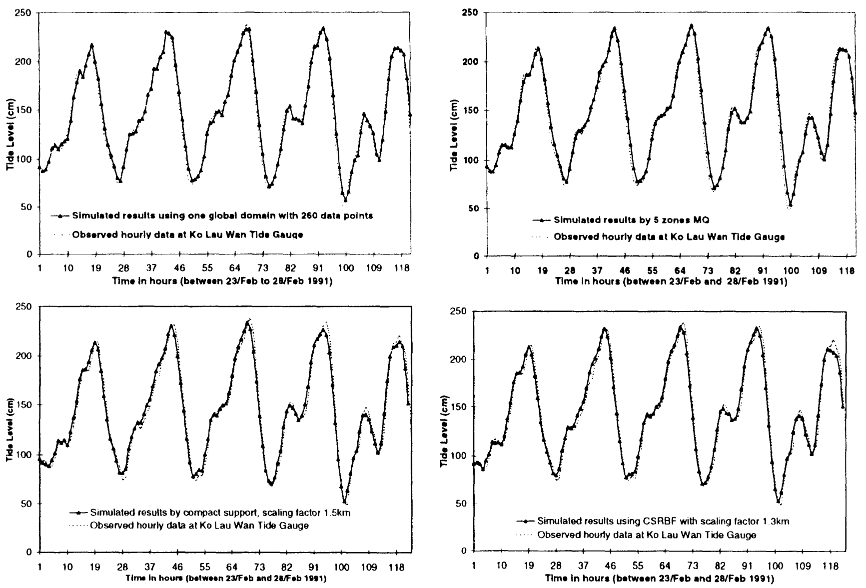

Figure 3: Comparison of the simulated results with the observed hourly tidal level in Tolo Harbour from 23 Feb to 28 Feb 1991.

5 Conclusion and Discussion

Both compact support and multizone decomposition techniques make the RBFs more feasible for solving large-scale problems. The numerical examples have demonstrated an improvement in computational efficiency without significant degradation in accuracy provided a suitable scaling factor is used for CSRBF or the multizone system is well designed.

CSRBFs approximation scheme is a relatively simple algorithm. The degree of accuracy of the simulated results is very much dependent on the size of the local support. To enhance the accuracy of the computations, large scaling factor δ could be used to increase the support for the function, however this would result in more intensive computation. Our numerical experiments showed that using variable δ could alleviate the problem of using a large support over the global domain. These two schemes do not require the use of iterative corrections scheme to remedy smoothness across

Transactions on Modelling and Simulation vol 22, © 1999 WIT Press, www.witpress.com, ISSN 1743-355X

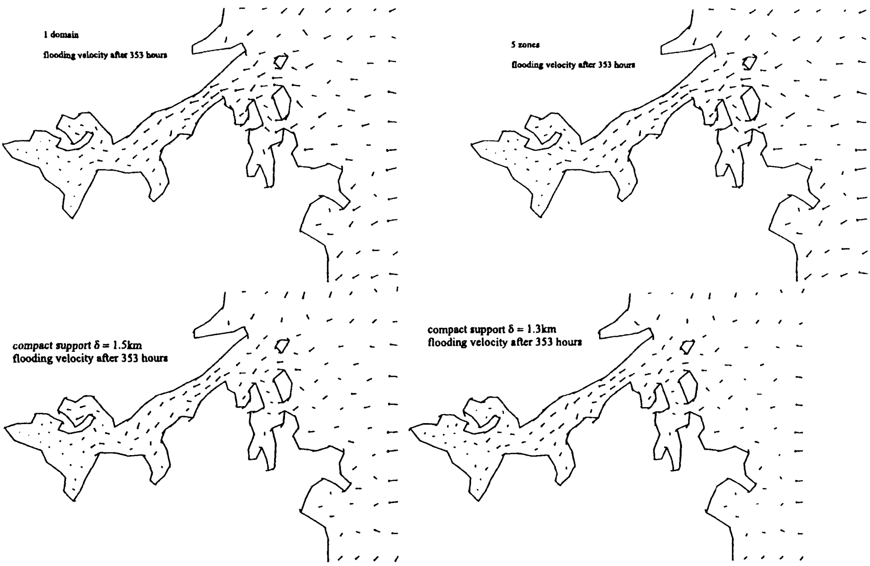

Figure 4: Distribution of the flood velocities in Tolo Harbour at 353 hours

boundaries which means more the computational cost. Multizone decomposition approach also lends itself well to parallel computation with multiple processors, where parallelization across zones are possible

References

[1] Anita S.M. Wong, Y.C. Hon, S.L. Chung, K.C. Ho "A Computational Model for Monitoring Water Quality and Ecological Impacts in Marine Environments", *J. of Appl. Science & Comput.*, Vol. 4, No.1, pp. 75-97, 1997.

[2] S.M. Wong, Y.C. Hon, T.S. Li, S.L. Chung and E.J. Kansa "Multi-zone decomposition for simulation of time-dependent problems using the Multiquadric scheme", to appear at the *J. Comput. & Math. with Applic.*

[3] M.J.D Powell, "The theory of radial basis function approximation in 1990", Chapter 3, *Wavelets, subdivision algorithm and radial basis functions*, ed. Will Light, Vol. II, *Oxford University Press,* pp. 105-210, 1992.

[4] H. Wendland, "Piecewise polynomial, positive definite and compactly compacted radial functions of minimal degree", *J. Adv. in Comput. Math.* No. 4, pp. 389-396, 1995.

[5] Zongmin Wu, "Positive definite radial functions with compact support", *J. Adv. in Comput. Math.* No. 4, pp. 283-292, 1995.

[6] M. S. Floater and A. Iske, "Multistep scattered data interpolation using compactly supported radial basis functions ", *J. Comput. Applied Math.* No. 73, pp. 65-78, 1996.

[7] Gregory E. Fasshauer, "On smoothing for multilevel approximation with radial basis functions", to appear at the *Proceeding of 9th Int. Conference on Approx. Theory,* Nashville, TN, 1998.

[8] Gregory E. Fasshauer, "Solving differential equations with radial basis functions: Multilevel methods nd smoothing", to appear at the *J. Adv. in Comput. Math.*